International Journal of Thermophysics, Vol. 19, No. 2, 1998

Measurements of Thermal Conductivity and Thermal Diffusivity of CVD Diamond[1]

J. E. Graebner[2]

The thermal conductivity κ of natural, gem-quality diamond, which can be as high as 2500 $Wm^{-1} K^{-1}$ at 25°C, is the highest of any known material. Synthetic diamond grown by chemical vapor deposition (CVD) of films up to 1 mm thick exhibits generally lower values of κ, but under optimal growth conditions it can rival gem-quality diamond with values up to 2200 $Wm^{-1} K^{-1}$. However, it is polycrystalline and exhibits a columnar microstructure. Measurements on free-standing CVD diamond, with a thickness in the range 25–400 μm, reveal a strong gradient in thermal conductivity as a function of position z from the substrate surface as well as a pronounced anisotropy with respect to z. The temperature dependence of κ in the range 4 to 400 K has been analyzed to determine the types and numbers of phonon scattering centers as a function of z. The defect structure, and therefore the thermal conductivity, are both correlated with the microstructure. Because of the high conductivity of diamond, these samples are thermally thin. For example, laser flash data for a 25-μm-thick diamond sample is expected to be virtually the same as laser flash data for a 1-μm-thick fused silica sample. Several of the techniques described here for diamond are therefore applicable to much thinner samples of more ordinary material.

KEY WORDS: chemical vapor deposition (CVD) diamond; phonon scattering; specific heat; thermal conductivity; thermal diffusivity.

1. INTRODUCTION

Gem-quality single crystals of diamond are well known to have the highest thermal conductivity of any known substance for temperatures above roughly 50 K. With the advent in the past 5 years of chemical vapor deposition (CVD) diamond films up to 1000 μm thick, the question of the conductivity of these polycrystalline films has received a great deal of

[1] Invited paper presented at the Thirteenth Symposium on Thermophysical Properties, June 22–27, 1997, Boulder, Colorado, U.S.A.

[2] Bell Labs, Lucent Technologies, Murray Hill, New Jersey 07974, U.S.A.

0195-928X/98/0300-0511$15.00/0

attention. The conductivity has turned out to span an order of magnitude, ranging from 2200 $Wm^{-1} K^{-1}$ down to several hundred $Wm^{-1} K^{-1}$ in a way that depends on the preparation conditions and the resulting microstructure and impurity content. The films exhibit a local conductivity which is anisotropic and which has a gradient with respect to z, the distance in the film from the substrate side. This behavior is correlated with the columnar microstructure and, in this respect, may be qualitatively similar to many other thin or thick films. We review here how such properties may be deduced from relatively simple measurements with essentially one-dimensional heat flow.

Most of the measurements were performed on samples in the range 3 to 500 μm thick. Some samples were polished by the manufacturer but most were as-grown, with a rough growth surface and a roughness of the order of 10% of the total film thickness. Rectangular bars 5 to 10 mm long were laser-cut by the manufacturer to give very precise and parallel edges. Most samples were free-standing, the substrate having been etched away, but some thin films (3 to 13 μm) were only partially free-standing.

The microstructure of CVD diamond is typically columnar. After random nucleation, the film grows by competitive growth of randomly oriented crystallites. The crystallites with the fastest-growing orientation soon dominate, resulting in columns of nearly parallel grains. The direction of fastest growth is usually $\langle 110 \rangle$, though under certain growth conditions it is $\langle 100 \rangle$. The in-plane dimensions of the grains grow monotonically, although not linearly, with z. Microscopic examination of CVD diamond films [1] has shown the presence of microcracks in some grain boundaries, as well as a general tendency of impurities and defects to be clustered at or near grain boundaries [2].

2. MEASUREMENT TECHNIQUES

We describe briefly four techniques used to measure the in-plane ($\kappa_{||}$) or perpendicular ($\kappa_{\perp}$) conductivity, or diffusivity ($D_{||}$ or $D_{\perp}$). We use the definition $D = \kappa/C$, where C is the heat capacity per unit volume. The latter has been measured [3] for CVD diamond films greater than 300 μm and found to be within 1% of the bulk value, justifying the common practice of using published data for C in bulk single crystals to convert measured values of κ to values of D, or vice versa, in CVD diamond. For thinner films, C undoubtedly falls somewhat below the bulk value due to porosity of the material in the earliest stages of growth. A mass density of several percent below the bulk value has been observed [4] for $z \approx 30\,\mu$m, so that precise measurements of conductivity/diffusivity in thin films would require corrections for this effect.

The loss of heat from a sample by radiation is a well known problem for thermal measurements. In many cases, this source of error can be reduced by decreasing the dimensions or changing the geometry. While the high conductivity of diamond tends to minimize such problems, we include radiation in the following discussion for the purpose of maintaining the highest accuracy.

Most of the measurements described here were conducted with an experimental arrangement designed to achieve one-dimensional heat flow, either parallel or perpendicular to the plane of the sample. This has the advantage of simplifying the data analysis by reducing one's reliance on complicated mathematical models, which often do not accurately take into account all aspects of the heat flow.

2.1. Two-Heater Heated Bar

The thermal conductivity of rectangular bars of CVD diamond was measured with a high accuracy with a technique [1] which uses two thin-film heaters evaporated directly onto a sample, one near each end, as shown in Fig. 1. Temperatures between the heaters were measured by a row of four or more thermocouples made with very fine wire, with a precision of 0.001°C. Measurements were performed with the sample in vacuum, surrounded by a copper shield at T_0, the temperature of the thermal ground. With heat generated only in the heater near the thermally grounded end, and in the absence of radiative heat loss, the rest of the sample attained a uniform temperature a degree or so above T_0. The presence of any radiative heat loss was indicated by a small temperature gradient along the sample, providing a highly sensitive and quantitative test for radiative loss. Power P was then applied instead to the heater at the free end to generate a thermal gradient. The measured gradient could be corrected accurately for radiative loss, if any, and used as dT/dx to calculate $\kappa = P/(AdT/dx)$, where $A = ZW$ was the cross-sectional area perpendicular to the heat flow, and Z and W were the thickness and width, respectively. W was defined by the highly parallel (laser-cut) edges, so that the overall estimated uncertainty in κ was approximately 3%, dominated by the variation in Z along a typical sample.

2.2. Thin Window

For CVD diamond films in the range of 3–13 μm grown on silicon substrates, the in-plane conductivity was measured [5] by etching away the substrate in a small area, 2×4 mm, leaving a free-standing window of diamond, and using thin-film heater and thermocouples to perform a

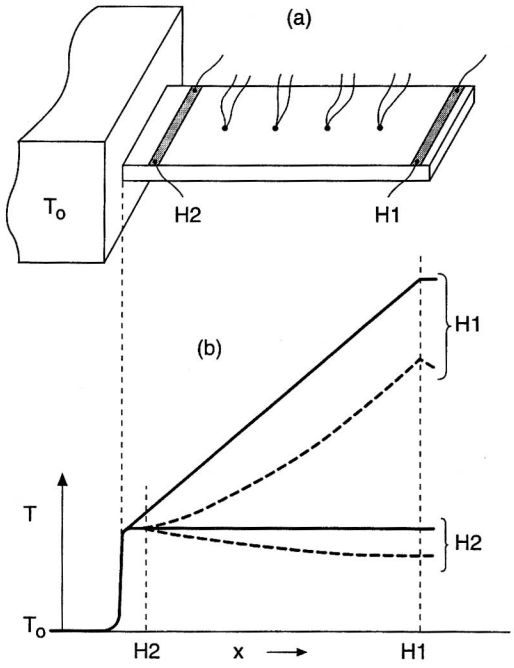

Fig. 1. Two-heater heated bar technique. The thermal ground is a copper block at temperature T_o. Heater H2 provides a sensitive test for loss of heat by radiation, while heater H1 is used to measure the thermal conductivity. Solid lines, zero radiation loss; dashed lines, severe radiation loss.

steady-state measurement. The thin-film thermocouples were calibrated with thin-wire thermocouples attached as indicated in Fig. 2. The measured thermal profile was numerically fitted by a two-dimensional calculation of Poisson's equation with the known heater as the source term. (A longer window in the direction of the heater would make the heat flow more one-dimensional, minimizing end effects.) The fit provided a value for $\kappa_{||}$. The best fit was obtained with window dimensions slightly larger than actual, indicating some finite thermal impedance between the film and the substrate.

The dimensions of the window were chosen to be small enough to reduce any radiative loss of heat to less than 1% of the heat conducted in the plane of the film from the heater to thermal ground. For films of other material with a lower conductivity, several options are available. One could reduce the scale still further, as the error due to radiation goes as the

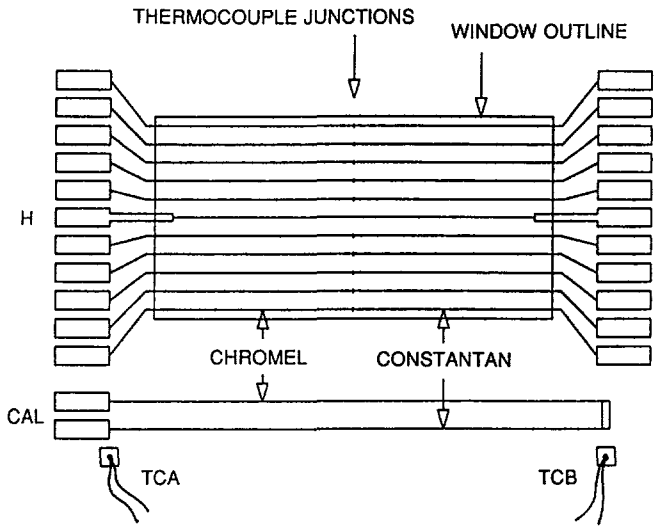

Fig. 2. The pattern of the heater (H), thermocouples, and gold contact pads (closed rectangular outlines) deposited on the surface of a diamond film in the vicinity of a window in the silicon substrate. Also shown is a calibration thermocouple. Wire thermocouples TCA and TCB are used to measure the temperature gradient imposed from right to left by an external heater while the voltage at CAL is monitored.

square of the window dimension in the direction of heat flow. Alternatively, one could use AC heating and study the frequency dependence of the phase and amplitude of the thermal waves generated by the heater, effectively using the Angstrom technique, which is more often used with a sample in the shape of a long bar. With the appropriate combination of phase and amplitude measurements at several locations, the effects of radiation can be made to cancel out [6–8].

2.3. Laser Flash

A laser-flash method was used to measure the thermal diffusivity $D_\perp$ for heat flow in the direction perpendicular to the plane of the sample [9]. A 5-ns pulse of a doubled Nd:YAG laser was used to heat one face of a sample that was coated on each face with a 300-nm-thick layer of sputtered Ti. The arrival of the diffusive pulse at the far face was detected by fast (100-MHz-bandwidth) infrared detection of thermal radiation from the second Ti layer. Typical results and a fit to the one-dimensional diffusion equation are shown in Fig. 3. Signal averaging was necessary to keep the temperature rise to a small value (less than 0.5°C) to assure that the

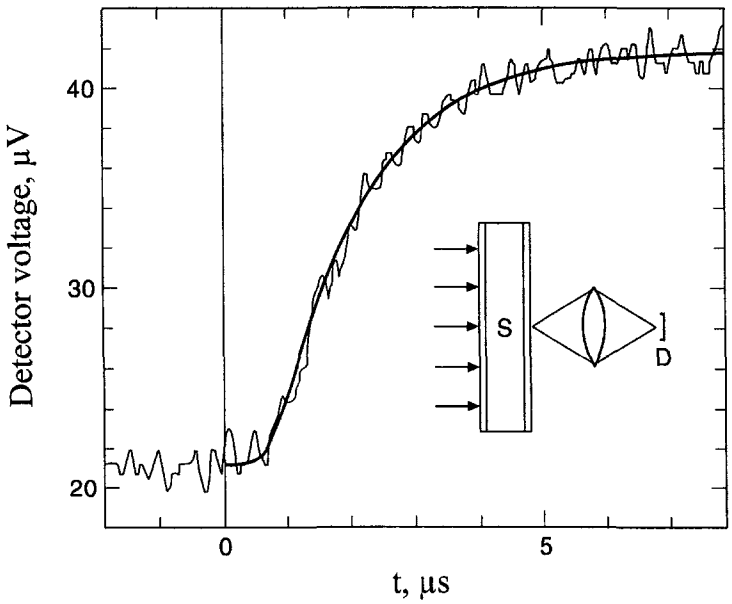

Fig. 3. Typical laser-flash data for CVD diamond, 300 μm thick. The laser pulse occurs at time 0, and the total rise in temperature observed with the infrared detector is 0.3°C. The solid curve is a least-squares fit to the one-dimensional diffusion equation. The inset shows the sample (S) coated on both sides with Ti. A germanium lens on the right collects infrared radiation for the detector (D).

average temperature of the sample was not significantly higher than its steady-state value.

The straightforward solution to the one-dimensional diffusion equation [10] assumes an impulse of energy at the front face. In practice, this requires that the pulse length be no longer than 1–2% of $t_{1/2}$, the time taken for the pulse to diffuse far enough through the sample that the temperature of the rear face rises to half its final value. Specifically, $t_{1/2} = 1.38Z^2/(\pi^2 D_\perp)$, where Z is the sample thickness. With a pulse width of 5 ns, this imposes a lower limit on Z of approximately 25 μm for diamond films, which for this thickness typically have $D_\perp = 3\ \mathrm{cm^2\ s^{-1}}$. Use of this technique on thinner samples of diamond would require either a shorter laser pulse or a calculation of the effects of a finite pulse. The influence of thin layers of Ti would also need to be investigated both theoretically and experimentally.

High-diffusivity materials such as diamond are the most difficult to measure with the laser flash technique. The characteristic time of the measurement, $t_{1/2} \propto Z^2/D_\perp$, shows that for more typical materials with

diffusivities of the order of 0.01 $cm^2 s^{-1}$, the same pulse length could be used with samples as thin as 1 μm, preferably of an opaque material so that no Ti absorbing/radiating layers are needed.

2.4. Transient Thermal Grating

In contrast with the above techniques, which average over the whole sample, there are a number of methods that provide a more local measurement near the surface of a sample. Among these, we discuss transient thermal gratings (TTG). A thermal grating consists of a pattern of parallel lines of higher temperature created on the surface of a sample by the interference pattern of two coherent laser beams intersecting at a small angle with respect to each other. The spacing Λ of the lines can be adjusted, typically in the range 10 to 1000 μm, by adjusting the angle of intersection. The exponential decay of the temperature amplitude of the grating is a direct measure of the diffusivity $D_{||}$ in the plane of the surface and at right angles to the thermal lines [11]. The decay of the amplitude can be monitored by diffraction of a second laser beam, yielding an average of $D_{||}$ over the common area of the two beams (typically several square millimeters), or much more locally by examining the angle or temperature of a small spot on the order of 10 μm. An example of the latter is shown in Fig. 4 for a thin

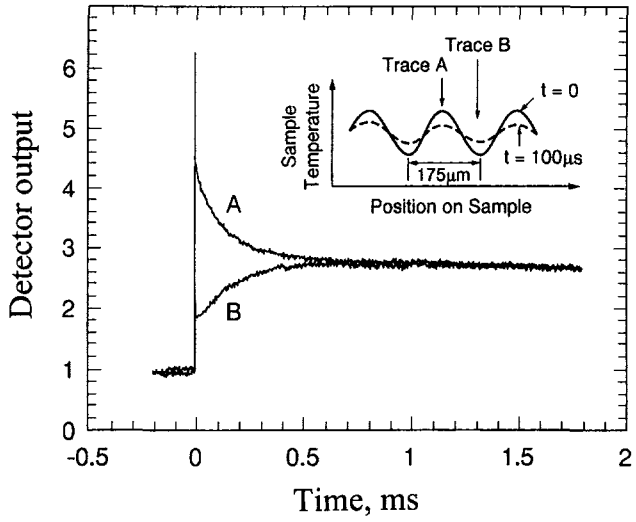

Fig. 4. Two traces (superimposed) of the infrared detector output when the detection spot is located on a peak (trace A) or a valley (trace B) of a transient thermal grating with wavelength $\Lambda = 175$ μm. The sample is a 6.5-μm-thick foil of Ti. The laser pulse occurs at time $t = 0$.

sample of Ti foil [12]. The spatial resolution of the spot under investigation is typically 20 μm. The temperature-vs-time data for peaks or valleys of the thermal grating show clearly the decay of the grating, from which the diffusivity is calculated. The Ti is thermally uniform on this scale, but data have been obtained for CVD diamond which shows nonsmooth behavior at some grain boundaries [13].

The depth of penetration of the grating is approximately Λ/π below the surface [11], so that the depth over which $D_{||}$ is averaged is under the control of the experimenter. The TTG technique is particularly useful for high-temperature investigation of thin films, especially free-standing, as the effects of radiation can be made negligibly small by using small values of Λ.

3. RESULTS AND EXTRACTION OF A LOCAL CONDUCTIVITY

The above techniques and others have been used to measure the properties of many samples of CVD diamond. Typically, black samples have a thermal conductivity of 5 to 8 W cm^{-1} K^{-1} that is roughly temperature independent in the range 25 to 125°C, while the clearest specimens have values in the range 18 to 22 W cm^{-1} K^{-1} at 25°C and decrease with increasing temperature. Of particular interest is a series of samples which showed a dependence on thickness, as described below.

In order to investigate the effect of the z-dependent microstructure on the thermal properties without cutting or grinding, and possibly damaging, the sample, a series of samples was prepared at Crystallume, Inc., in five runs during which the growth conditions were kept as constant as possible. The different growth times resulted in five samples in the range of 28 to 350 μm in thickness, which were assumed to have nearly identical microstructural profiles as a function of z. The conductivity $\kappa_{||}$ averaged over each sample (measured by the heated-bar technique) was found to increase strongly with thickness Z, as shown in Fig. 5. Because of this positive thickness dependence, it was clear that the upper portion of each sample had a higher local conductivity than the lower portion of the same sample. One can easily deduce a local conductivity from the sample-averaged data in Fig. 5 by the following procedure. Comparing two adjacent samples, the conductance ($Z\kappa_{||}$) of the thinner sample is the same as the conductance of the same portion of the thicker sample. The conductance of the upper portion (remainder) of the thicker sample is therefore the total conductance of the thicker sample minus the total conductance of the thinner. This procedure yields a local conductance, averaged over only the upper portion of the thicker sample. The local conductivity calculated in this way from successive pairs of samples is shown in Fig. 5. Alternatively, the local conductivity can be derived analytically by the following approach: the observed

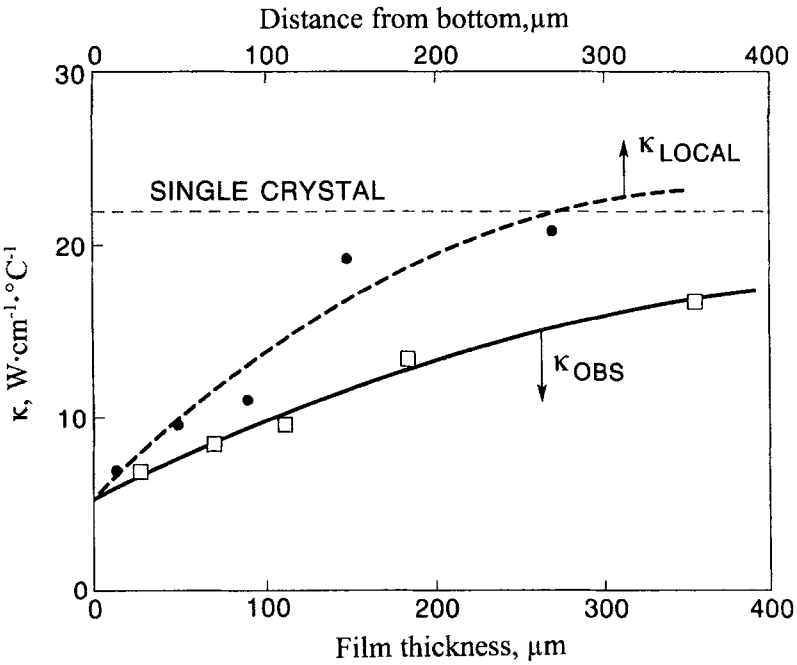

Fig. 5. Measured thermal conductivity $\kappa_{||}$ at 25°C for five samples of CVD diamond. The local conductivity is derived in two ways (see text), resulting in the filled circles and the dashed curve. The line labeled "single crystal" indicates the typical conductivity reported for high-quality (Type IIa) bulk diamond.

parallel conductivity can be approximated as $\kappa_{obs} = A_0 + A_1 Z + A_2 Z^2$, and the local conductivity can be calculated as $\kappa_{local} = \partial(Z\kappa_{obs})/\partial Z = A_0 + 2A_1 Z + 3A_2 Z^2$. The results (Fig. 5) are consistent with the discrete differentiation procedure described above. The local conductivity at 25°C is thus seen to increase by a factor of more than four from the bottom of the thickest sample to the top, and the value near the top rivals the conductivity of the best single-crystal diamond.

Measurements of the *perpendicular* diffusivity were performed on a similar set of carefully prepared samples of different thicknesses in order to determine a local value of $\kappa_\perp$. Again, the observed $D_\perp$ showed a positive thickness dependence, and a local value was found by an analogous procedure, which, however, was modified for the case of layers of diamond in series, rather than in parallel as above. The results for the local $\kappa_\perp$, as well as the local $\kappa_{||}$, are shown in Fig. 6. The z dependence of the two quantities is quite different, implying an anisotropy of as much as a factor of two in the range $z = 30$ to $100\,\mu$m. If we assume that phonon scattering (thermal

resistance) occurs primarily at grain boundaries where lattice defects tend to collect, the schematic in Fig. 6 suggests that the gradient in conductivity as a function of z is due to the growth of the average grain size with z and that the anisotropy is related to the columnar shape of the grains.

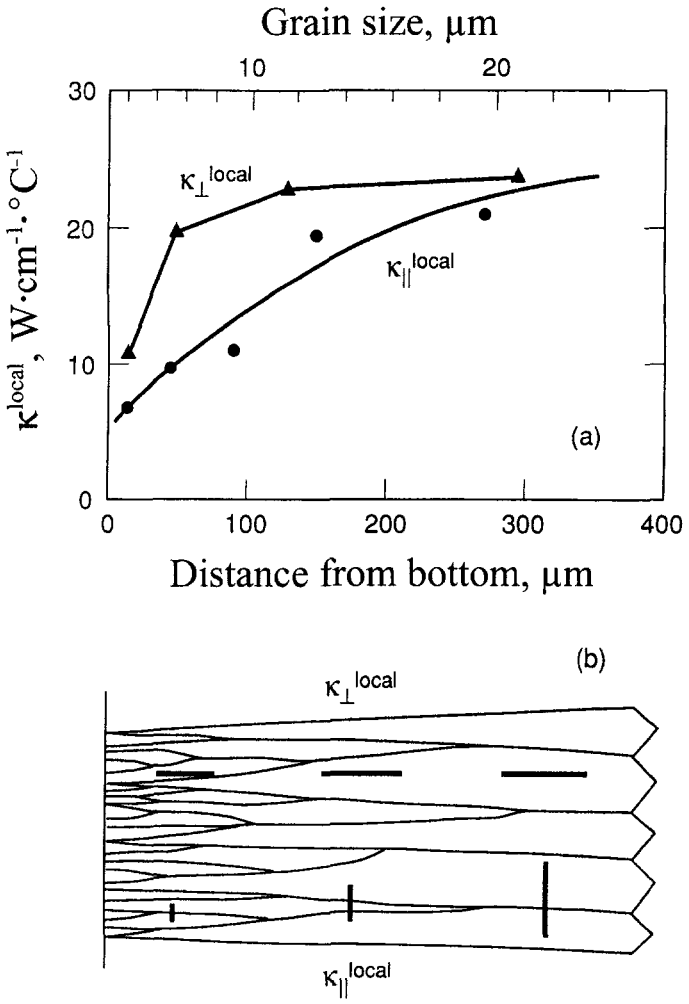

Fig. 6. (a) Local conductivity for heat flow perpendicular to the film, $\kappa_{\perp}^{local}$, compared with that for heat flow parallel to the film, $\kappa_{||}^{local}$. The nonlinear top scale gives the grain size as a function of distance from the bottom of the samples (bottom scale). (b) Schematic view of the typical cone-shaped grain structure of CVD diamond films. The lengths of the bars are proportional to local conductivity for heat flow in the two directions.

4. ANALYSIS OF PHONON SCATTERING

To determine the source of thermal resistance, it is often very useful to measure the conductivity over a large temperature range and to fit the data with a model which includes a number of phonon scattering mechanisms. Such measurements [14] in CVD diamond were performed for the same five samples over the range 4 to 400 K. The theoretical model includes intrinsic phonon–phonon scattering as well as phonon scattering from

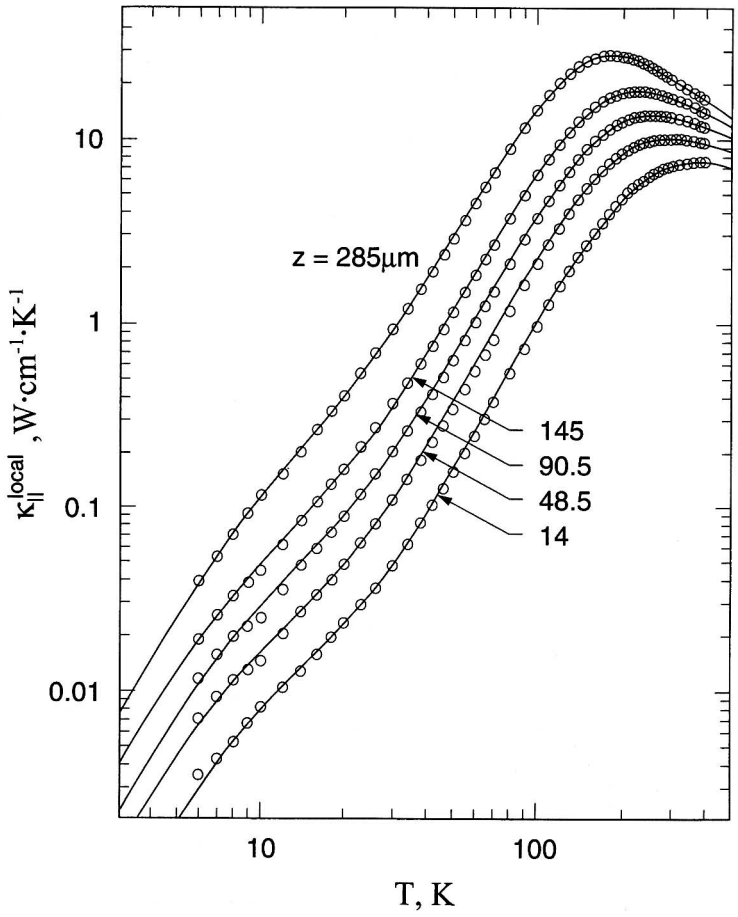

Fig. 7. The local conductivity $\kappa_{||}{}^{local}(z, T)$ for different heights z above the substrate derived from measurements on five samples of CVD diamond over a wide temperature range. The curves through the data are calculated with a theoretical model of thermal conductivity using phonon scattering parameters adjusted for optimum fit.

point defects, extended defects, and dislocations. Each of these sources of scattering has its own temperature dependence and tends to contribute most strongly only in certain temperature ranges. By applying the procedure described above for the room temperature conductivity, a local conductivity can be extracted at each temperature and the local conductivity vs temperature at a given height z above the substrate (Fig. 7) can

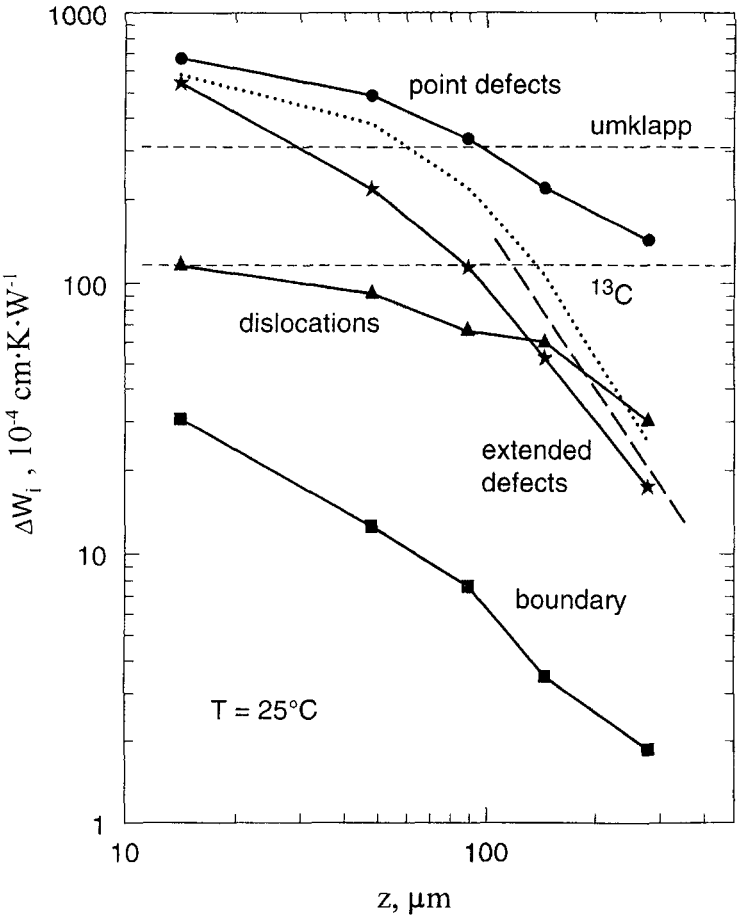

Fig. 8. Approximate contributions to the thermal resistivity ($=\kappa^{-1}$) of point defects, extended defects, dislocations, and boundary scattering at room temperature, as a function of the distance z from the substrate face. The upper horizontal dashed line indicates the resistivity due to phonon–phonon processes, and the lower horizontal dashed line that due to point-defect scattering from the natural abundance of ^{13}C. The dotted curve shows the point-defect resistivity after subtraction of the natural ^{13}C contribution.

be analyzed for phonon scattering mechanisms. The results for each mechanism can be plotted vs z to exhibit the z dependence of the concentration of point defects, extended (diameter, ≈ 15 Å) defects, and dislocations (Fig. 8). The anisotropy in the thermal conductivity shown in Fig. 6 can be understood quantitatively [14] if the point defects and extended defects are all located at or near grain boundaries and if the dislocations are oriented primarily along the columnar axes. Microscopic information (such as TEM) on the presence of point defects, extended defects, and dislocations as a function of z is now needed for an even more detailed understanding of the thermal resistance in CVD diamond.

REFERENCES

1. J. E. Graebner, M. E. Reiss, L. Seibles, T. M. Hartnett, R. P. Miller, and C. J. Robinson, *Phys. Rev.* **B50**:3702 (1994).
2. A. V. Hetherington, C. J. H. Wort, and P. Southworth, *J. Mater. Res.* **5**:1591 (1990).
3. J. E. Graebner, *Diamond Relat. Mater.* **5**:1366 (1996).
4. J. E. Graebner, J. A. Mucha, and F. A. Baiocchi, *Diamond Relat. Mater.* **5**:682 (1996).
5. J. E. Graebner, J. A. Mucha, L. Seibles, and G. W. Kammlott, *J. Appl. Phys.* **71**:3143 (1992).
6. R. W. King, *Phys. Rev.* **6**:437 (1915).
7. P. H. Sidles and G. C. Danielson, *J. Appl. Phys.* **25**:58 (1954).
8. C. Starr, *Rev. Sci. Instrum.* **8**:61 (1937).
9. J. E. Graebner, S. Jin, G. W. Kammlott, J. A. Herb, and C. F. Gardinier, *Nature* **359**:401 (1992).
10. H. S. Carslaw and J. C. Jaeger, *Conduction of Heat in Solids* (Clarendon Press, 1959).
11. O. W. Kading, E. Matthias, R. Zachai, H.-J. Fusser, and P. Munzinger, *Diamond Relat. Mater.* **2**:1185 (1993).
12. J. E. Graebner, *Rev. Sci. Instrum.* **66**:3903 (1995).
13. H. Verhoeven, private communication (1996).
14. J. E. Graebner, S. Jin, J. A. Herb, and C. F. Gardinier, *J. Appl. Phys.* **76**:1552 (1994).